Inorg. Chem. **2007**, *46*, 6702–6714

Linear Metal–Metal-Bonded Tetranuclear M–Mo–Mo–M Complexes (M = Ir and Rh): Oxidative Metal–Metal Bond Formation in a Tetrametallic System and 1,4-Addition Reaction of Alkyl Halides

Masato Ohashi, Asuka Shima, Tobias Rüffer, Hitoshi Mizomoto, Yutaka Kaneda, and Kazushi Mashima*

Department of Chemistry, Graduate School of Engineering Science, Osaka University, Toyonaka, Osaka 560-8531, Japan

Received December 26, 2006

Reaction of $Mo_2(pyphos)_4$ (**1**) with $[MCl(CO)_2]_2$ (M = Ir and Rh) afforded linear tetranuclear complexes of a formula $Mo_2M_2(CO)_2(Cl)_2(pyphos)_4$ (**2**, M = Ir; **3**, M = Rh). X-ray diffraction studies confirmed that two "MCl(CO)" fragments are introduced into both axial sites of the Mo_2 core in **1** and coordinated by two PPh_2 groups in a trans fashion, thereby forming a square-planar geometry around each M(I) metal. Treatment of **2** and **3** with an excess amount of ^{t}BuNC and XylNC induced dissociation of the carbonyl and chloride ligands to yield the corresponding dicationic complexes $[Mo_2M_2(pyphos)_4(^t\text{BuNC})_4](Cl)_2$ (**5a**, M = Ir; **6a**, M = Rh) and $[Mo_2M_2(pyphos)_4(\text{XylNC})_4](Cl)_2$ (**7**, M = Ir; **8**, M = Rh). Their molecular structures were characterized by spectroscopic data as well as X-ray diffraction studies of BPh_4 derivatives $[Mo_2M_2(pyphos)_4(^t\text{BuNC})_4](BPh_4)_2$ (**5b**, M = Ir; **6c**, M = Rh), which confirmed that there is no direct σ-bonding interaction between the M(I) atom and the Mo_2 core. The M(I) atom in **5** and **6** can be oxidized by either 2 equiv of $[Cp_2Fe][PF_6]$ or an equimolar amount of I_2 to afford $Mo(II)_2M(II)_2$ complexes, $[Mo_2M_2(X)_2(^t\text{BuNC})_4(pyphos)_4]^{2+}$ in which two Mo–M(II) single bonds are formed and the bond order of the Mo–Mo moiety has been decreased to three. The Ir(I) complex **5a** reacted not only with methyl iodide but also with dichloromethane to afford the 1,4-oxidative addition products $[Mo_2Ir_2(CH_3)(I)(^t\text{BuNC})_4(pyphos)_4](Cl)_2$ (**13**) and $[Mo_2Ir_2(CH_2Cl)(Cl)(^t\text{BuNC})_4(pyphos)_4](Cl)_2$ (**15**), respectively, although the corresponding reactions using the Rh(I) analogue **6** did not proceed. Kinetic analysis of the reaction with CH_3I suggested that the 1,4-oxidative addition to the Ir(I) complex occurs in an S_N2 reaction mechanism.

Introduction

Multinuclear transition-metal complexes are currently attracting great interest because of their fundamental bonding nature[1] as well as their promising applicability to homo- and heterogeneous catalysts for organic synthesis,[2] extensive electronic and optoelectronic materials,[3] and supramolecular chemistry.[4] Covalently bonded metal strings, in particular, have emerged as an active research area. Polydentate ligands such as oligo-α-pyridylamido,[5−7] polyene,[8] dpmp [bis(diphenylphosphanylmethyl)phenylphosphane],[9,10] and dmb (1,8-diisocyano-*p*-menthane)[11] have been utilized as supporting ligands, and partial oxidation of d^8 square-planar complexes[12,13] or partial reduction of d^7 metal compounds[14,15] has also been developed to form metal−metal-bonded linear metal clusters, e.g., platinum blue.

For metal−metal-bonded clusters, the electronic environment, which depends on the metals used and their oxidation state, predominates their bonding nature and unique properties, including chemical reactivity. In particular, linear

* To whom correspondence should be addressed. E-mail: mashima@chem.es.osaka-u.ac.jp.

(1) Cotton, F. A.; Walton, R. A. *Multiple Bonds Between Metal Atoms*, 2nd ed.; Clarendon Press: Oxford, U.K., 1993.

(2) (a) *Catalysis by Di- and Polynuclear Metal Cluster Complexes*; Adams, R. D., Cotton, F. A., Eds.; Wiley-VCH: New York, 1998. (b) *Metal Clusters in Catalysis*; Gates, B. C., Guzci, L., Knozinger, V. H., Eds.; Elsevier: Amsterdam, 1986. (c) *Metal-Metal Bonds and Clusters in Chemistry and Catalysis*; Fackler, J. P., Ed.; Plenum: New York, 1990.

(3) (a) Böhn, M. C. *One-Dimensional Organometallic Materials*; Springer: New York, 1987. (b) Bruce, D. W.; O'Hara, D. *Inorganic Materials*; Wiley: New York, 1992. (c) Miller, J. S. *Extended Linear Chain Compounds*; Plenum: New York, 1982; Vols. 1−3. (d) Bera, J. K.; Dunbar, K. R. *Angew. Chem., Int. Ed.* **2002**, *41*, 4453.

(4) (a) Lehn, J.-M. *Supramolecular Chemistry*: *Concepts and Perspective*; VCH: New York, 1995 (b) Cotton, F. A.; Lin, C.; Murillo, C. A. *Acc. Chem. Res.* **2001**, *34*, 759. (c) Leininger, S.; Olenyuk, B.; Stang, P. J. *Chem. Rev.* **2000**, *100*, 853. (d) Fujita, M. *Chem. Soc. Rev.* **1998**, *27*, 417.

10.1021/ic062474q CCC: $37.00
Published on Web 07/03/2007

heterometallic clusters, especially those composed of both early and late transition metals, are different from homopolynuclear complexes because of the electronic anisotropy arising between the metals. Although there have been many studies on the synthesis and reactivity of linear polynuclear transition-metal complexes, few attempts have been made to achieve heteronuclear clusters.[10,16] Incorporation of many different elements into a well-designed polydentate ligand as a coordination site would allow the arrangement of more than two types of transition metals in a linear manner. Thus, our efforts have been made to align transition metals by using a tridentate ligand, 6-diphenylphosphino-2-pyridonate (abbreviated as pyphos), in which three elements, P, N, and O, are linearly located over the rigid pyridone framework. The trans-arranged PPh_2 groups in both axial positions of the paddle-wheel-type complex, $Mo_2(pyphos)_4$ (**1**),[17] which was synthesized by a ligand exchange reaction with $Mo_2(OCOCH_3)_4$, possess superior capability to bind two additional metal atoms to give a M−Mo−Mo−M framework. By using the quadruply bonded dimolybdenum complex **1** as a core part of the metal strings, we demonstrated the construction of linear heterometallic clusters containing both group 6 and group 10 metals such as $Mo_2Pd_2Cl_2(pyphos)_4$.[18]

We are interested in the versatility of metal−metal bond formations as well as their reaction mechanism in our heteronuclear tetranuclear system. Although metal−metal bond formations have been given by one-electron oxidation of each terminal metal in dinuclear complexes having no metal−metal bond,[19−27] comparable studies on multinuclear

(5) Recent references: (a) Berry, J. F.; Cotton, F. A.; Lu, T.; Murillo, C. A. *Inorg. Chem.* **2003**, *42*, 4425. (b) Berry, J. F.; Cotton, F. A.; Lu, T.; Murillo, C. A.; Wang, X. *Inorg. Chem.* **2003**, *42*, 3595. (c) Berry, J. F.; Cotton, F. A.; Lei, P.; Lu, T.; Murillo, C. A. *Inorg. Chem.* **2003**, *42*, 3534. (d) Berry, J. F.; Cotton, F. A.; Daniels, L. M.; Murillo, C. A.; Wang, X. *Inorg. Chem.* **2003**, *42*, 2418. (e) Berry, J. F.; Cotton, F. A.; Lei, P.; Murillo, C. A. *Inorg. Chem.* **2003**, *42*, 377. (f) Berry, J. F.; Cotton, F. A.; Daniels, L. M.; Murillo, C. A. *J. Am. Chem. Soc.* **2002**, *124*, 3212. (g) Clérac, R.; Cotton, F. A.; Daniels, L. M.; Dunbar, K. R.; Murillo, C. A.; Wang, X. *Inorg. Chem.* **2001**, *40*, 1256. (h) Clérac, R.; Cotton, F. A.; Jeffery, S. P.; Murillo, C. A.; Wang, X. *Inorg. Chem.* **2001**, *40*, 1265. (i) Clérac, R.; Cotton, F. A.; Daniels, L. M.; Dunbar, K. R.; Murillo, C. A.; Pascual, I. *Inorg. Chem.* **2000**, *39*, 748. (j) Clérac, R.; Cotton, F. A.; Daniels, L. M.; Dunbar, K. R.; Murillo, C. A.; Pascual, I. *Inorg. Chem.* **2000**, *39*, 752. (k) Clérac, R.; Cotton, F. A.; Dunbar, K. R.; Lu, T.; Murillo, C. A.; Wang, X. *J. Am. Chem. Soc.* **2000**, *122*, 2272. (l) Clérac, R.; Cotton, F. A.; Daniels, L. M.; Dunbar, K. R.; Kirschbaum, K.; Murillo, C. A.; Schultz, A. J.; Wang, X. *J. Am. Chem. Soc.* **2000**, *122*, 6226.

(6) Recent references: (a) Lin, S.-Y.; Chen, I.-W. P.; Chen, C.-H.; Hsieh, M.-H.; Yeh, C.-Y.; Lin, T.-W.; Chen, Y.-H.; Peng, S.-M. *J. Phys. Chem. B* **2004**, *108*, 959. (b) Yeh, C.-Y.; Chiang, Y.-L.; Lee, G.-H.; Peng, S.-M. *Inorg. Chem.* **2002**, *41*, 4096. (c) Yeh, C.-Y.; Chou, C.-H.; Pan, K.-C.; Wang, C.-C.; Lee, G.-H.; Su, Y. O.; Peng, S.-M. *J. Chem. Soc., Dalton Trans.* **2002**, 2670. (d) Peng, S.-M.; Wang, C.-C.; Jang, Y.-L.; Chen, Y.-H.; Li, F.-Y.; Mou, C.-Y.; Leung, M.-K. *J. Magn. Magn. Mater.* **2000**, *209*, 80.

(7) van Albada, G. A.; van Koningsbruggen, P. J.; Mutikainen, I.; Turpeinen, U.; Reedijk, J. *Eur. J. Inorg. Chem.* **1999**, 2269.

(8) (a) Tatsumi, Y.; Naga, T.; Nakashima, H.; Murahashi, T.; Kurosawa, H. *Chem. Commun.* **2004**, 1430. (b) Murahashi, T.; Uemura, T.; Kurosawa, H. *J. Am. Chem. Soc.* **2003**, *125*, 8436. (c) Murahashi, T.; Higuchi, Y.; Katoh, T.; Kurosawa, H. *J. Am. Chem. Soc.* **2002**, *124*, 14288. (d) Murahashi, T.; Nagai, T.; Mino, Y.; Mochizuki, E.; Kai, Y.; Kurosawa, H. *J. Am. Chem. Soc.* **2001**, *123*, 6927. (e) Murahashi, T.; Nagai, T.; Okuno, T.; Matsutani, T.; Kurosawa, H. *Chem. Commun.* **2000**, 1689.

(9) Balch, A. L. In *Progress in Inorganic Chemistry*; Karlin, K. D., Ed.; John Wiley & Sons: New York, 1994; Vol. 41, p 239 and references therein.

(10) (a) Goto, E.; Begum, R. A.; Zhan, S.; Tanase, T.; Tanigaki, K.; Sakai, K. *Angew. Chem., Int. Ed.* **2004**, *43*, 5029. (b) Tanase, T.; Begum, R. A.; Toda, H.; Yamamoto, Y. *Organometallics* **2001**, *20*, 968. (c) Tanase, T.; Begum, R. A. *Organometallics* **2001**, *20*, 106. (d) Tanase, T.; Ukaji, H.; Takahata, H.; Toda, T.; Igoshi, T.; Yamamoto, Y. *Organometallics* **1998**, *17*, 196. (e) Tanase, T.; Toda, H.; Yamamoto, Y. *Inorg. Chem.* **1997**, *36*, 1571.

(11) (a) Zhang, T.; Drouin, M.; Harvey, P. D. *Inorg. Chem.* **1999**, *38*, 1305. (b) Zhang, T.; Drouin, M.; Harvey, P. D. *Inorg. Chem.* **1999**, *38*, 957.

(12) Examples for platinum compounds: (a) Matsumoto, K.; Sakai, K. *Adv. Inorg. Chem.* **2000**, *49*, 375. (b) Lippert, B. *Coord. Chem. Rev.* **1999**, *182*, 263. (c) Sakai, K.; Tanaka, Y.; Tsuchiya, Y.; Hirata, K.; Tsubomura, T.; Iijima, S.; Bhattacharjee, A. *J. Am. Chem. Soc.* **1998**, *120*, 8366. (d) Sakai, K.; Takeshita, M.; Tanaka, Y.; Ue, T.; Yanagisawa, M.; Kosaba, M.; Tsubomura, T.; Ato, M.; Nakano, T. *J. Am. Chem. Soc.* **1998**, *120*, 11353. (e) Matsumoto, K.; Sakai, K.; Nishio, K.; Tokisue, Y.; Ito. R.; Nishide, T.; Schichi, Y. *J. Am. Chem. Soc.* **1992**, *114*, 8110. (f) Sakai, K.; Matsumoto, K. *J. Am. Chem. Soc.* **1989**, *111*, 3074. (g) Bernardinelli, G.; Castan, P.; Soules, R. *Inorg. Chim. Acta* **1986**, *120*, 205. (h) Ginsberg, A. P.; O'Halloran, T. V.; Fanwick, P. E.; Hollis, L. S.; Lippard, S. J. *J. Am. Chem. Soc.* **1984**, *106*, 5430. (i) Lippard, S. J. *Science* **1982**, *218*, 1075.

(13) Examples for rhodium and iridium compounds: (a) Tejel, C.; Ciriano, M. A.; Villarroya, B. E.; López, J. A.; Lahoz, F. J.; Oro, L. A. *Angew. Chem., Int. Ed.* **2003**, *42*, 530. (b) Tejel, C.; Ciriano, M. A.; Villarroya, B. E.; Gelpi, R.; López, J. A.; Lahoz, F. J.; Oro, L. A. *Angew. Chem., Int. Ed.* **2001**, *40*, 4084. (c) Tejel, C.; Ciriano, M. A.; López, J. A.; Lahoz, F. J.; Oro, L. A. *Angew. Chem., Int. Ed.* **1998**, *37*, 1542. (d) Ciriano, M. A.; Sebastián, S.; Oro, L. A.; Tiripicchio, A.; Tiripicchio-Camellini, M. *Angew. Chem., Int. Ed.* **1988**, *27*, 402. (e) Mann, K. R.; DiPierro, M. J.; Gill, T. P. *J. Am. Chem. Soc.* **1980**, *102*, 3965.

(14) Examples for infinite Rh−chain compounds: (a) Pruchnik, F. P.; Jakimowicz, P.; Ciunik, Z.; Stanislawek, K.; Oro, L. A.; Tejel, C.; Ciriano, M. A. *Inorg. Chem. Commun.* **2001**, *4*, 19. (b) Prater, M. E.; Pence, L. E.; Clérac, R.; Finnis, G. M.; Campana, C.; Auban-Senzier, P.; Jérome, D.; Canadell, E.; Dunbar, K. R. *J. Am. Chem. Soc.* **1999**, *121*, 8005. (c) Finnis, G. M.; Canadell, E.; Campana, C.; Dunbar, K. R. *Angew. Chem., Int. Ed.* **1996**, *35*, 2772.

(15) Pruchnik, F. P.; Jakimowicz, P.; Ciunik, Z. *Inorg. Chem. Commun.* **2001**, *4*, 726.

(16) Examples for linear heterometallic cluster: (a) Clérac, R.; Cotton, F. A.; Dunbar, K. R.; Murillo, C. A.; Wang, X. *Inorg. Chem.* **2001**, *40*, 420. (b) Cotton, F. A.; Murillo, C. A.; Roy, L. E.; Zhou, H.-C. *Inorg. Chem.* **2000**, *39*, 1743. (c) Balch, A. L.; Catalano, V. J.; Noll, B. C.; Olmstead. M. M. *J. Am. Chem. Soc.* **1990**, *112*, 7558. (d) Balch, A. L.; Catalano, V. J.; Olmstead, M. M. *J. Am. Chem. Soc.* **1990**, *112*, 2010. (e) Balch, A. L. *Pure Appl. Chem.* **1988**, *60*, 555.

(17) Mashima, K.; Nakano, H.; Nakamura, A. *J. Am. Chem. Soc.* **1993**, *115*, 11632.

(18) (a) Mashima, K.; Nakano, H.; Nakamura, A. *J. Am. Chem. Soc.* **1996**, *118*, 9083. (b) Mashima, K.; Tanaka, M.; Tani, K.; Nakamura, A.; Mori, W.; Takeda, S.; Yamaguchi, K. *J. Am. Chem. Soc.* **1998**, *120*, 12151.

(19) (a) Tejel, C.; Ciriano, M. A.; López, J. A.; Lahoz, F. J.; Oro, L. A. *Organometallics* **1997**, *16*, 4718. (b) Ciriano, M. A.; Pérez-Torrente, J. J.; Oro, L. A. *J. Organomet. Chem.* **1993**, *445*, 273. (c) Fernández, M. J.; Modrego, J.; Lahoz, F. J.; López, J. A.; Oro, L. A. *J. Chem. Soc., Dalton Trans.* **1990**, 2587. (d) Oro, L. A.; Pinillos, M. T.; Tiripicchio, A.; Tiripicchio-Camellini, M. *Inorg. Chim. Acta* **1985**, *99*, L13.

(20) (a) Balch, A. L.; Hunt, C. T.; Lee, C.-L.; Olmstead, M. M.; Farr, J. P. *J. Am. Chem. Soc.* **1981**, *103*, 3764. (b) Balch, A. L.; Labadie, J. W.; Delker, G. *Inorg. Chem.* **1979**, *18*, 1224. (c) Balch, A. L. *J. Am. Chem. Soc.* **1976**, *98*, 8049.

(21) (a) He, X. D.; Maisonnat, A.; Dahan, F.; Poilblanc, R. *Organometallics* **1991**, *10*, 2443. (b) El Amane, M.; Maisonnat, A.; Dahan, F.; Poilblanc, R. *New J. Chem.* **1988**, *12*, 661.

(22) (a) Bushnell, G. W.; Fjeldsted, D. O. K.; Stobart, S. R.; Wang, J. *Organometallics* **1996**, *15*, 3785. (b) Atwood, J. L.; Beveridge, K. A.; Bushnell, G. W.; Dixon, K. R.; Eadie, D. T.; Stobart, S. R.; Zaworotko, M. J. *Inorg. Chem.* **1984**, *23*, 4050.

(23) Schmidbaur, H.; Franke, R. *Inorg. Chim. Acta* **1975**, *13*, 85.

(24) Cotton, F. A.; Lahuerta, P.; Latorre, J.; Sanau, M.; Solana, I.; Schwotzer, W. *Inorg. Chem.* **1988**, *27*, 2131.

(25) Finke, R. G.; Gaughan, G.; Plerpont, C.; Noordlk, J. H. *Organometallics* **1983**, *2*, 1481.

(26) Kubiak, C. P.; Woodcock, C.; Eisenberg, R. *Inorg. Chem.* **1980**, *19*, 2733.

(27) Janke, C. J.; Tortorelli, L. J.; Burn, J. L. E.; Tucker, C. A.; Woods, C. *Inorg. Chem.* **1986**, *25*, 4597.

complexes composed of more than three transition metals are relatively rare.[5d,f] Preliminary results obtained for the first synthesis of novel tetranuclear Rh−Mo−Mo−Rh arrays and oxidation of Rh(I) atoms to Rh(II) atoms, which induced formation of Rh−Mo bonds, were reported earlier,[28] and an extended and full account of the synthesis and reactivity of linearly aligned tetranuclear complexes bearing the M(I)···Mo(II)−Mo(II)···M(I) skeleton (M = Ir and Rh) is presented here. We found that one-electron oxidation of the terminal M(I) metals in these complexes by oxidants, such as ferrocenium cation or I_2, results in formation of the corresponding complexes with an M(II)−Mo(II)−Mo(II)−M(II) framework with concomitant formation of two M−Mo bonds. In addition to the oxidation reaction, the present work also discloses new oxidative addition reactions of alkyl halides such as methyl iodide and dichloromethane toward the Ir(I) complexes, resulting in an alternative Mo−Ir bond formation to yield novel 1,4-oxidative addition products. Their reaction mechanism will also be discussed.

Results

Synthesis and Characterization of Linear Tetranuclear M_2Mo_2 Complexes [M = Ir(I) and Rh(I)]. Treatment of **1** with 1 equiv of $[IrCl(CO)_2]_2$,[29] which was derived from in situ carbonylation of $[IrCl(coe)_2]_2$, resulted in clean formation of $[Mo_2Ir_2(CO)_2(Cl)_2(pyphos)_4]$ (**2**) as a red-purple solid in 94% yield (eq 1). The rhodium analogue $[Mo_2Rh_2(CO)_2(Cl)_2(pyphos)_4]$ (**3**)[28] was synthesized in a similar manner using $[RhCl(CO)_2]_2$ instead of $[IrCl(CO)_2]_2$.

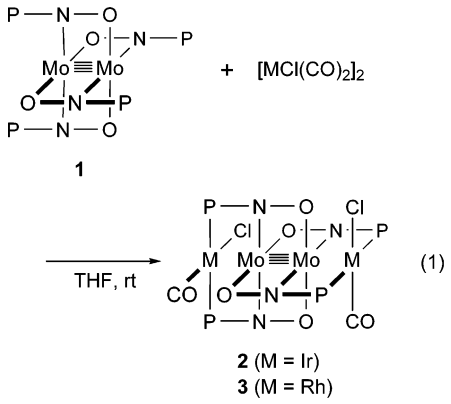

Complexes **2** and **3** were fully characterized on the basis of the ^1H and ^{31}P NMR, IR, and mass spectroscopies, and their molecular structures were confirmed by the X-ray diffraction studies. Although the four pyridonate ligands of **1** were spectroscopically observed as equivalent, the corresponding resonances observed in the ^1H NMR spectra of **2** and **3** appeared as two sets of inequivalent signals, presumably due to coordination of two different ligands, CO and Cl, to each terminal metal. This finding is consistent with the fact that the $^{31}P\{^1H\}$ NMR spectrum of **3** displayed two doublets at δ 25.8 and 25.9 with the same coupling constant (J_{RhP} = 120 Hz), the value of which was almost the same as that of the mononuclear complexes, *trans*-RhCl(CO)$(PPh_3)_2$ (J_{RhP} = 129 Hz) and *trans*-RhCl(CO)$(PyPPh_2)_2$ (J_{RhP} = 127 Hz).[30] Four PPh_2 groups of the iridium complex **2**, however, were incidentally equivalent and observed as a singlet at δ 21.7.

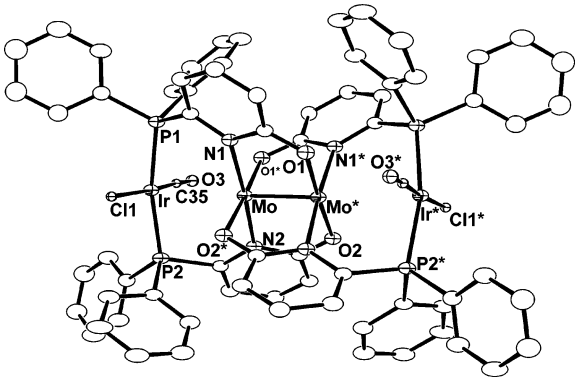

Figure 1. Molecular structure of **2** with thermal ellipsoids at the 30% probability level. H atoms and solvents are omitted for clarity.

Table 1. Selected Bond Lengths [Å] and Angles [deg] for **2** and **3**[a]

	2 (M = Ir)	**3** (M = Rh)
Mo−Mo*	2.1115(9)	2.1087(7)
Mo···M	2.8727(5)	2.8746(5)
M−P1	2.3218(13)	2.3292(12)
M−P2	2.3262(14)	2.3244(12)
M−C35	1.762(9)	1.951(7)
M−Cl1	2.361(4)	2.3931(17)
Mo−O1	2.108(4)	2.089(3)
Mo−O2	2.093(4)	2.104(3)
Mo−N1	2.166(4)	2.155(4)
Mo−N2	2.156(4)	2.163(4)
Mo−Mo···M	176.10(3)	175.71(2)
C35−M−P1	93.3(3)	86.5(2)
C35−M−P2	87.3(3)	95.2(2)
Cl1−M−P1	84.40(8)	95.55(5)
Cl1−M−P2	95.55(8)	84.03(5)
Mo···M−P1	84.50(3)	83.12(3)
Mo···M−P2	83.41(3)	84.30(3)
Mo···M−C35	88.9(3)	92.6(2)
Mo···M−Cl1	93.60(8)	92.82(4)

[a] Symmetry transformations used to generate equivalent atoms (*): $-x$, y, $0.5 - z$.

Readily discernible vibrations associated with the CO ligands of **2** and **3** were observed at 1986 and 1996 cm^{-1}, respectively. These values are slightly higher than those of the corresponding mononuclear *trans*-MCl(CO)$(PPh_3)_2$ complexes (M = Ir, 1953 cm^{-1}; M = Rh, 1962 cm^{-1}),[31] reflecting the decrease in electron density at the terminal M centers in **2** and **3**.

Crystals of **2** and **3** suitable for X-ray crystallography were grown from their dichloromethane solutions layered with ether. Both compounds were isomorphic, and the molecular structure of **2** is shown in Figure 1. The selected bond distances and angles for **2** and **3** are listed in Table 1. The CO and Cl ligands coordinated to each iridium atom in complex **2** were found to be disordered, presumably because

(28) Rüffer, T.; Ohashi, M.; Shima, A.; Mizomoto, H.; Kaneda, Y.; Mashima, K. *J. Am. Chem. Soc.* **2004**, *126*, 12244.
(29) Roberto, D.; Cariati, E.; Psaro, R.; Ugo, R. *Organometallics* **1994**, *13*, 4227.
(30) Farr, J. P.; Olmstead, M. M.; Hunt, C. H.; Balch, A. L. *Inorg. Chem.* **1981**, *20*, 1182.
(31) Garrou, P. E.; Hartwell, G. E. *Inorg. Chem.* **1976**, *15*, 646−650.

their positions alternated randomly throughout the crystal. These ligands were modeled satisfactorily with the population of 0.5 to 0.5.

The X-ray diffraction studies clearly demonstrated that linearly aligned M−Mo−Mo−M tetrametal cores are supported by four pyphos ligands. Two "*trans*-M(CO)(Cl)" fragments are located at both axial positions of the Mo−Mo bond, and the four metal centers are linearly arranged as evident from the Mo−Mo−M bond angle (**2**, 176.10(3)°; **3**, 175.71(2)°). Mo−Mo bond distances of 2.1115(9) (**2**) and 2.1087(7) Å (**3**) are comparable to those observed for the quadruply bonded $Mo(II)_2$ complexes such as the parent complex **1** (2.098(2) Å),[18a] $Mo_2(L)_4$ (L = μ-acetate, 2.0934(8) Å; L = 6-methylpyridonate, 2.065(1) Å),[32] and M′(I)···Mo−Mo···M′(I) complexes (M′(I) = Pd and Pt, 2.095(4)−2.101(2) Å).[18a] As expected for the d^8 M(I) complexes, the Rh(I) and Ir(I) ions have a square-planar geometry with the sum of the angles of L−M−L′ (L,L′ = C35, Cl1, P1, and P2) being 360.55° for **2** and 361.28° for **3**. All Mo−M−P angles are acute due to the steric strain derived from the rigid pyridonate framework of the ligand. Thus, it is assumed that there are no direct σ-bond interactions between the Mo_2 core and the terminal metal, although the interatomic Mo−Ir distance of 2.8727(5) Å for **2** and the interatomic Mo−Rh distance of 2.8746(5) Å for **3** fall within the range normally associated with the corresponding Mo−M single bonds.[33,34]

When complex **1** was reacted with a 1:1 mixture of $[RhCl(CO)_2]_2$ and $[IrCl(CO)_2]_2$ a mixed-metal tetranuclear complex, $[Mo_2IrRh(CO)_2(Cl)_2(pyphos)_4]$ (**4**), was formed along with the concomitant formation of homometal complexes **2** and **3** (eq 2). Complex **4** could not be isolated, but its structure was characterized based on the $^{31}P\{^1H\}$ NMR spectrum, which displayed two new resonances at δ 23.5 (s) and 28.9 (d, J_{RhP} = 114 Hz) assignable to the phosphorus nuclei bound to Ir and those bound to Rh, respectively. When equal amounts of the isolated complexes **2** and **3** were dissolved in CD_2Cl_2 at ambient temperature a possible comproportionation reaction from **2** and **3** to **4** did not proceed, strongly indicating that **2** and **3** are stable enough and do not release the terminal "M(CO)(Cl)" fragments in solution.

1 + 0.5 $[RhCl(CO)_2]_2$ + 0.5 $[IrCl(CO)_2]_2$

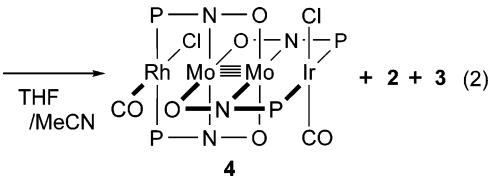

4

Although we expected that oxidation of the M(I) atoms of **2** and **3** to M(II) atoms results in formation of M−Mo bonds, oxidation of **3** by ferrocenium cation resulted in its decomposition by release of CO. Thus, we prepared the isocyanide derivatives of **2** and **3** to improve the stability as well as the solubility of the complex.

Addition of an excess amount of ^{t}BuNC to an acetonitrile solution of **2** at room temperature caused an immediate change of color from reddish purple to dark blue, giving a dicationic complex $[Mo_2Ir_2(^t\text{BuNC})_4(pyphos)_4](Cl)_2$ (**5a**) in quantitative yield (eq 3). During the reaction both a carbonyl ligand and a chlorine atom attached to the terminal Ir atom were substituted by isocyanide ligands to afford the dicationic complex **5a**, where the chlorine atoms were eliminated from the coordination sphere of the iridium centers. Introduction of four isocyanide ligands was confirmed based on the disappearance of the carbonyl stretching vibration (1986 cm^{-1}) and appearance of the N≡C stretching vibration (2154 cm^{-1}) as well as a single proton resonance due to four *tert*-butyl groups (δ 0.78, 36 H). In the $^{31}P\{^1H\}$ NMR spectrum of **5a** a single resonance assignable to four PPh_2 groups bound to the iridium centers was observed at δ 19.8. Chlorine anions of **5a** were replaced by adding $NaBPh_4$ in methanol to give $[Mo_2Ir_2(^t\text{BuNC})_4(pyphos)_4](BPh_4)_2$ (**5b**). These dicationic complexes **5a** and **5b** did not dissolve in nonpolar solvents such as pentane, toluene, and benzene but were soluble in acetonitrile and THF.

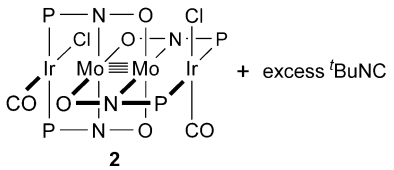

2

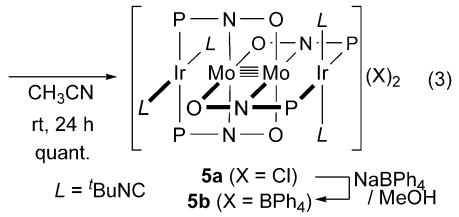

The rhodium *tert*-butyl isocyanide analogue $[Mo_2Rh_2(^t\text{BuNC})_4(pyphos)_4](X)_2$ (**6a**, X = Cl; **6b**, X = PF_6; **6c**, X = BPh_4) was previously prepared using a similar reaction, and

(32) (a) Cotton, F. A.; Mester, Z. C.; Webb, T. R. *Acta Crystallogr.* **1974**, *B30*, 2768. (b) Cotton, F. A.; Fanwick, P. E.; Niswander, R. H.; Sekutowski, J. C. *J. Am. Chem. Soc.* **1978**, *100*, 4725.

(33) The Rh−Mo bond distances found in Rh−Mo complexes were ca. 2.77−2.95 Å. (a) Du, S.; Kautz, J. A.; McGrath, T. D.; Stone, F. G. A. *Inorg. Chem.* **2002**, *41*, 3202. (b) Ikada, T.; Mizobe, Y.; Hidai, M. *Organometallics* **2001**, *20*, 4441. (c) Ikada, T.; Kuwata, S.; Mizobe, Y.; Hidai, M. *Inorg. Chem.* **1999**, *38*, 64. (d) Coutinho, K. J.; Dickson, R. S.; Fallon, G. D.; Jackson, W. R.; Simone, T. D.; Skelton, B. W.; White, A. H. *J. Chem. Soc., Dalton Trans.* **1997**, 3193. (e) Cano, M.; Heras, J. V.; Ovejero, P.; Pinilla, E.; Monge, A. *J. Organomet. Chem.* **1991**, *410*, 101. (f) Winter, G.; Schulz, B.; Trunschke, A.; Miessner, H.; Böttcher, H.-C.; Walther, B. *Inorg. Chim. Acta* **1991**, *184*, 27. (g) Mague, J. T.; Johnson, M. P. *Organometallics* **1990**, *9*, 1254. (h) Lo Schiavo, S.; Faraone, F.; Lanfranchi, M.;Tiripicchio, A. *J. Organomet. Chem.* **1990**, *387*, 357. (i) Farrugia, L. J.; Miles, A. D.; Stone, F. G. A. *J. Chem. Soc., Dalton Trans.*, **1984**, 2415. (j) Finke, R. G.; Gaughan, G.; Pierpont, C.; Cass, M. E. *J. Am. Chem. Soc.* **1981**, *103*, 1399.

(34) The Ir−Mo bond distances found in Ir−Mo complexes were ca. 2.77−2.95 Å. (a) Jin, G.-X.; Wang, J.-Q.; Zheng, C.; Weng, L.-H.; Herberhold, M. *Angew. Chem., Int. Ed.* **2005**, *44*, 259−262. (b) Usher, A. J.; Humphrey, M. G.; Wills, A. C. *J. Organomet. Chem.* **2003**, *682*, 41−48. (c) Seino, H.; Masunori, T.; Hidai, N.; Mizobe, Y. *Organometallics* **2003**, *22*, 3424−3431. (d) Lucas, N. T.; Humphrey, M. G. *Acta. Crystallogr.* **2002**, *C58*, m171−m173. (e) McFariand, J. M.; Churchill, M. R.; See, R. F.; Lake, C. H.; Atwood, J. D. *Organometallics* **1991**, *10*, 3530−3537. (f) Albianti, A.; Togni, A.; Venanzi, L. M. *Organometallics* **1986**, *5*, 1785−1791.

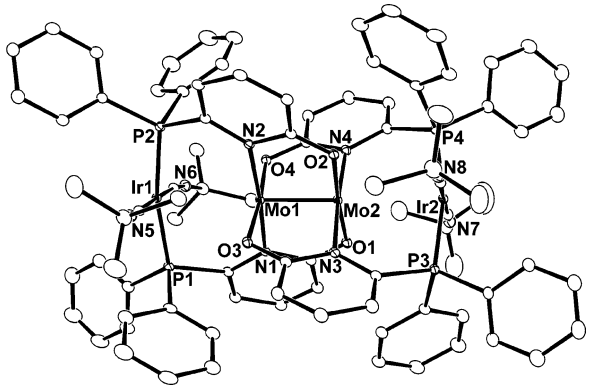

Figure 2. Molecular structure of **5b** with thermal ellipsoids at the 30% probability level. H atoms, counteranions, and solvents are omitted for clarity.

Table 2. Selected Bond Lengths [Å] and Angles [deg] for **5b** and **6c**

	5b (M = Ir)	**6c** (M = Rh)
Mo1−Mo2	2.1128(2)	2.1054(6)
Mo1···M1	2.8476(2)	2.8462(6)
Mo2···M2	2.8400(2)	2.8453(6)
M1−P1	2.3126(6)	2.3011(13)
M1−P2	2.3139(6)	2.3101(14)
M1−C1	1.967(3)	1.969(6)
M1−C6	1.978(3)	1.983(6)
M2−P3	2.3030(6)	2.3111(16)
M2−P4	2.3079(6)	2.3020(15)
M2−C11	1.957(3)	1.972(6)
M2−C16	1.969(3)	1.978(6)
Mo1−O3	2.0973(16)	2.105(4)
Mo1−O4	2.0903(17)	2.092(4)
Mo2−O1	2.0910(17)	2.105(3)
Mo2−O2	2.0999(17)	2.094(3)
Mo1−N1	2.174(2)	2.164(4)
Mo1−N2	2.175(2)	2.167(4)
Mo2−N3	2.1654(19)	2.180(5)
Mo2−N4	2.1742(19)	2.169(4)
Mo2−Mo1···M1	178.405(10)	179.02(3)
Mo1−Mo2···M2	178.876(11)	177.87(2)
C1−M1−P1	94.71(7)	85.93(15)
C1−M1−P2	86.30(7)	95.10(15)
C6−M1−P1	83.83(7)	94.10(16)
C6−M1−P2	95.01(7)	84.47(16)
C11−M2−P3	93.51(7)	86.31(16)
C11−M2−P4	86.77(8)	94.04(16)
C16−M2−P3	85.54(7)	95.13(17)
C16−M2−P4	94.44(7)	84.42(17)
Mo1···M1−P1	84.365(15)	84.45(4)
Mo1···M1−P2	85.150(15)	84.58(4)
Mo1···M1−C1	89.79(7)	90.42(15)
Mo1···M1−C6	89.41(7)	87.46(15)
Mo2···M2−P3	84.454(15)	83.72(4)
Mo2···M2−P4	84.805(15)	84.74(4)
Mo2···M2−C11	90.54(7)	88.09(16)
Mo2···M2−C16	90.79(7)	91.40(16)

the molecular structure was confirmed by the X-ray diffraction study of **6c**.[28] The molecular structure of **5b** was determined by X-ray analysis. The cationic part of **5b** is shown in Figure 2, and selected bond distances and angles of **5b** together with those of **6c**, whose structure is quite similar to that of **5b**, are listed in Table 2.

Rh and Ir atoms are located at both axial extensions of the Mo−Mo bond in **5b** and **6c**, respectively; the angles between the Mo1−Mo2 vector and the Mo1−M1 or the Mo2−M2 vectors were 178.405(10)° and 178.876(11)° for **5b** (M = Ir) and 179.02(3)° and 177.87(2)° for **6c** (M = Rh). M1 and M2 ions have a distorted square-planar geometry surrounded by two phosphorus atoms of the pyphos ligands and two terminal isocyanide ligands in trans arrangements. The square-planar geometry of each Ir(I) metal is perpendicular to the vector of the Mo_2 core. Substitution of the CO and Cl ligands in both **2** and **3** by ^{t}BuNC affects neither the Mo−Mo bond distances (**5b**, 2.1128(2) Å; **6c**, 2.1054(6) Å) nor the interatomic Mo−M distances (**5b**, 2.8476(2) and 2.8400(2) Å; **6c**, 2.8462(6) and 2.8453(6) Å). The sum of the four C−M−P angles around the terminal metal ion is 359.9° for Ir1 and 360.2° for Ir2, respectively, and the corresponding values for **6c** are 359.6° and 359.9°, though the P−M−P bond angles effectively deviate from linearity (**5b**, 169.46(2)° and 169.26(2)°; **6c**, 168.99(5)° and 168.44(5)°).

Reactions of **2** and **3** with an excess amount of XylNC instead of ^{t}BuNC also gave XylNC analogues **7** and **8** in excellent yields (eq 4). In the ^{1}H NMR and IR spectra of **7** the proton signal of the methyl groups and the N═C stretching vibration of the four XylNC ligands appeared at δ 1.75 ppm and 2172 cm^{-1}, respectively. The ^{31}P{^{1}H} NMR spectrum of **7** also displayed a singlet at δ 16.6, revealing that the four pyphos ligands are equivalent. The analytical data of the rhodium complex **8** also agree with incorporation of four XylNC molecules.

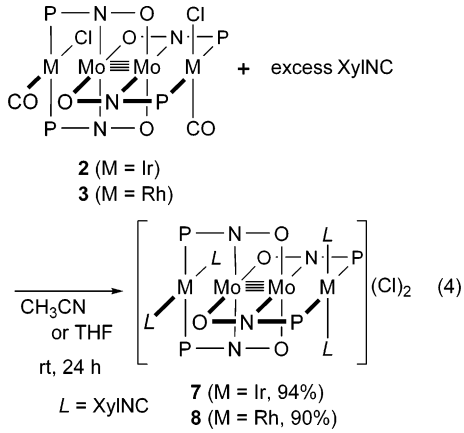

Oxidative M−Mo Bond Formation by Reaction of the Linear Tetranuclear Complexes 5a and 6a with [Cp_2Fe][PF_6] and I_2. Recently, we demonstrated that oxidation of each Rh(I) atom of **6a** by 2 equiv of [Cp_2Fe][PF_6] results in clean formation of [$Mo_2Rh_2(Cl)_2(^t$BuNC$)_4$(pyphos$)_4$][PF_6]$_2$ (**9a**) accompanied by formation of two Mo−Rh(II) single bonds and reduction in the bond order of the Mo−Mo moiety (Scheme 1a). The complete spectral assignment and molecular structure of **9a** have been reported.[28] A series of the halogen-substituted Rh(II) complexes [$Mo_2Rh_2(X)_2(^t$BuNC$)_4$(pyphos$)_4$][PF_6]$_2$ (**9b**, X = Br; **9c**, X = I) was quantitatively prepared by first treating complex **6a** with an excess amount of NaBr or KI followed by oxidation by 2 equiv of [Cp_2Fe][PF_6] (Scheme 1b).

In the UV−vis spectra of **9a**−**c** the absorption maxima (**9a**, λ 534 nm; **9b**, λ 578 nm; **9c**, λ 664 nm) of the MMCT

Scheme 1

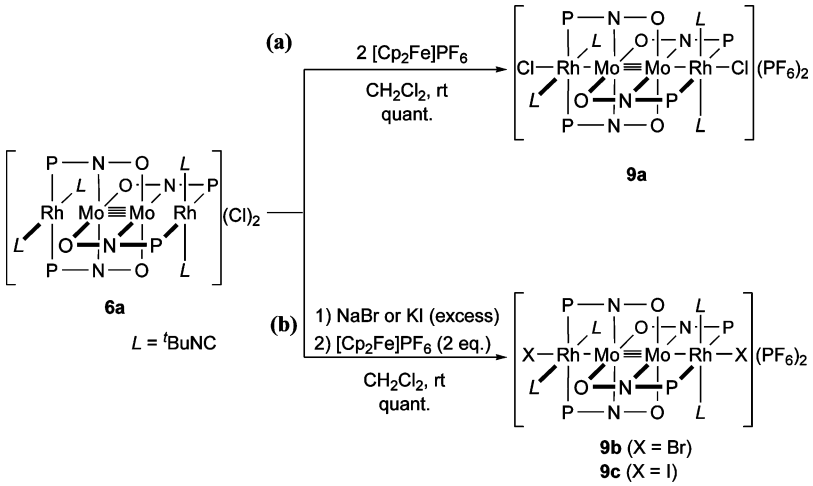

band depend on the halogen ligands and are red shifted in the order Cl < Br < I. The Raman active ν_{Mo-Mo} bands of **9a**−**c**, however, had almost the same wavenumber (**9a**, 388 cm^{-1}; **9b**, 389 cm^{-1}; **9c**, 387 cm^{-1}).

Interest in the correlation between the stability toward oxidation and the type of metal fragments introduced (Ir or Rh) into the terminal sites of the M−Mo−Mo−M fragment prompted us to measure the oxidation potentials of these tetranuclear isocyanide clusters. The cyclic voltammogram of the Mo_2Ir_2 complex **5a** measured in TBACl/MeCN solution at room temperature with a positively directed sweep showed a reversible, two-electron wave at −970 mV (vs Fc/Fc^+). This reversible event is indicative of an $Ir^{I}Ir^{I}/Ir^{II}Ir^{II}$ redox pair, clearly demonstrating that oxidation of **5a** is a more thermodynamically favorable process in comparison with that of **6a** (−660 mV vs Fc/Fc^+), which might explain the difference in the oxidative addition reactions between them (vide infra).

The iridium(I) analogue **5a** was readily oxidized by 2 equiv of ferrocenium cation to give the corresponding Ir(II)−Mo(II)−Mo(II)−Ir(II) complex, $[Mo_2Ir_2(Cl)_2(^tBuNC)_4(pyphos)_4](PF_6)_2$ (**10**) (eq 5), which was definitely identified on the basis of NMR spectroscopy as well as X-ray analysis.

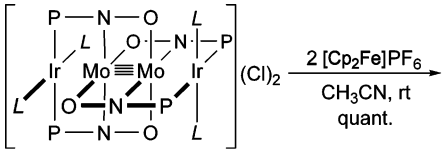

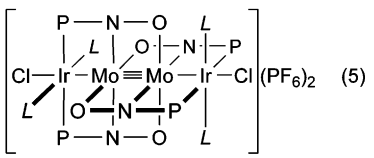

10 (5)

Suitable crystals of **10** for X-ray diffraction study were grown from a CH_2Cl_2/Et_2O solution. In the crystallographic unit cell of **10** a C_2 axis perpendicular to the Mo−Mo bond passes through the midpoint of two molybdenum atoms, and hence one-half is crystallographically unique. The ORTEP drawing of the cationic part of the iridium complex **10** is shown in Figure 3. The selected bond lengths and angles of **10** together with the rhodium−^{t}BuNC complex **9a**[28] are listed in Table 3.

The Cl−Ir−Mo−Mo−Ir−Cl skeleton of **10**, which was supported by four pyphos ligands, is almost linear [Mo−Mo−Ir, 179.78(3)°; Mo−Ir−Cl, 179.68(7)°]. The most notable structural feature of **10** is the octahedral geometry around each Ir atom, which is different from the square-planar geometry of **5b**. The Mo−Ir distance of **10** (2.7299(8) Å) is significantly shorter than that of **5b** (2.8476(2) and 2.8400(2) Å), while the Mo−Mo distance of 2.1283(14) Å is comparable to not only that of **5b** (2.1128(2) Å) but also that of the Pt−Mo≡Mo−Pt (2.134(1)−2.135(2) Å) and Pd−Mo≡Mo−Pd (2.119(2)−2.1221(9) Å) complexes.[18a]

The formal potential (−0.15 V vs Fc/Fc^+)[35] of I_2 as an oxidizing reagent is sufficient to oxidize the M(I) complexes. Treatment of **5a** and **6b** with an excess amount of I_2 resulted in 1,4-addition of I_2 to give the corresponding diiodo Ir(II) and Rh(II) complexes **11** and **9c** (Scheme 2a), respectively. When the XylNC complex **7** was successively treated with I_2 followed by $NaBPh_4$ an iodide complex, $[Mo_2Ir_2(I)_2(XylNC)_4(pyphos)_4](BPh_4)_2$ (**12**), was obtained (Scheme 2b). Complex **12** was isolated as a purple microcrystalline solid in 88% yield, and its structure was determined by X-ray analysis. The ORTEP drawing of the cationic part of **12** is shown in Figure 4. Selected bond lengths and angles of **12** are listed in Table 4.

Complex **12** crystallizes in monoclinic system *C*2/*c*. Its C_2 axis passes through the Ir(II)−Mo(II)−Mo(II)−Ir(II) tetrametal skeleton, and hence, all four metals are linearly aligned. Complex **12** essentially has the same stereochemical arrangement as complex **10**. The bond distances of Ir1−I1 and Ir2−I2 are 2.7760(8) and 2.7671(7) Å, respectively. The difference in the Ir−X bond distances between **12** (X = I) and **10** (X = Cl, 2.479(3) Å), despite the fact that the

(35) Connelly, N. G.; Geiger, W. E. *Chem. Rev.* **1996**, *96*, 877.

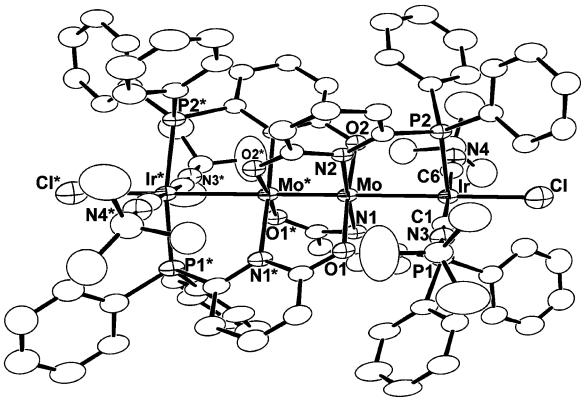

Figure 3. Molecular structure of **10** with thermal ellipsoids at the 30% probability level. H atoms, counteranions, and solvents are omitted for clarity.

Table 3. Selected Bond Lengths [Å] and Angles [deg] for **9a** and **10**[a]

	9a (M = Rh)	**10** (M = Ir)
Mo−Mo*	2.1239(10)	2.1283(14)
Mo−M	2.7307(7)	2.7299(8)
M−P1	2.3502(17)	2.342(2)
M−P2	2.3440(16)	2.340(2)
M−C1	1.984(7)	1.981(9)
M−C6	1.979(7)	1.980(9)
M−Cl1	2.477(2)	2.479(3)
Mo−O1	2.067(4)	2.082(5)
Mo−O2	2.075(4)	2.072(5)
Mo−N1	2.172(5)	2.164(6)
Mo−N2	2.167(5)	2.168(6)
Mo−Mo−M	179.77(3)	179.78(3)
Mo−M−Cl1	179.87(7)	179.68(7)
C1−M−P1	85.4(2)	95.2(2)
C1−M−P2	94.9(2)	84.3(2)
C6−M−P1	95.00(18)	85.1(3)
C6−M−P2	84.45(18)	95.3(3)
Cl1−M−C1	90.8(2)	90.5(3)
Cl1−M−C6	90.86(19)	89.9(3)
Cl1−M−P1	94.56(7)	94.41(9)
Cl1−M−P2	94.48(6)	94.64(8)
Mo−M−P1	85.44(4)	85.45(6)
Mo−M−P2	85.51(4)	85.50(5)
Mo−M−C1	89.07(19)	89.8(3)
Mo−M−C6	89.27(18)	89.8(3)

[a] Symmetry transformations used to generate equivalent atoms (*): $-x$, y, $0.5 - z$.

isocyanide ligand is different, reflects the difference between the covalent radii of the iodine atom and that of the chlorine atom.[36]

Each iridium ion has an octahedral geometry comprised of two phosphorus atoms, two XylNC ligands, one iodine atom, and one molybdenum atom. The Mo−Ir bond distances in **12** (2.7427(8) and 2.7161(8) Å) are significantly shorter than those of the Mo(II)···Ir(I) complexes **2** (2.8727(5) Å) and **5b** (av. 2.84 Å) but almost the same as that of the Mo(II)−Ir(II) complex **10** (2.7299(8) Å).

1,4-Oxidative Addition of MeI and CH_2Cl_2 toward $Mo(II)_2Ir(I)_2$ Isocyanide Complexes 5a and 7. The Ir(I) complexes **5a** and **7** immediately react with CH_3I, even though its redox potential[37] is too low to oxidize these Ir(I) complexes, at ambient temperature to afford $[Mo_2Ir_2(CH_3)(I)(^t$BuNC$)_4$(pyphos$)_4](Cl)_2$ (**13**) and $[Mo_2Ir_2(CH_3)(I)$(XylNC$)_4$(pyphos$)_4](Cl)_2$ (**14a**), respectively (eq 6). In sharp contrast, reaction of rhodium analogue **6a** did not proceed under the same conditions. Complexes **13** and **14a** were the products of a unique "1,4-oxidative addition" of methyl iodide, where one iridium atom is bound to the methyl group and the other is bound to iodide. In these reactions no intermediate species or homosubstituted Ir(II) products, such as diiodo and dimethyl complexes, were detected. Complexes **13** and **14a** were fully characterized on the basis of the ^{1}H and ^{31}P NMR, IR, and mass spectroscopies.

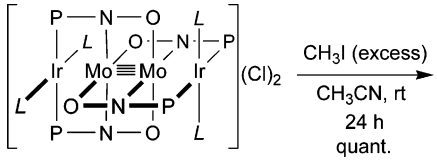

5a (L = ^{t}BuNC)
7 (L = XylNC)

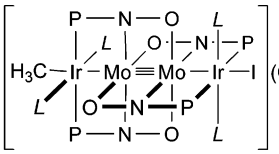

(6)

13 (L = ^{t}BuNC)
14a (L = XylNC)

As a consequence of the dissymmetric structure of **13**, its ^{31}P{^{1}H} NMR spectrum displayed two singlets at δ 0.9 and −1.1 due to phosphorus atoms bound to 'Ir−CH_3' and 'Ir−I', respectively. Furthermore, in the ^{1}H NMR spectrum of **13**, the Ir−CH_3 group was observed at δ 0.72 as a triplet (J_{PH} = 4.5 Hz, Figure 5a), which disappeared when labeled with CD_3I (Figure 5c). Reaction of **5a** with $^{13}CH_3I$ smoothly yielded an isotopomer of the Ir−$^{13}CH_3$ complex (**13-^{13}C**), whose ^{13}C{^{1}H} and ^{31}P{^{1}H} NMR spectra showed resonances at δ_C −27.9 (qt, J_{CH} = 136.2 Hz, J_{PC} = 2.4 Hz) and δ_P 0.9 with the same coupling constant as ^{13}C nuclei (d, J_{PC} = 2.4 Hz, Figure 5d). In Figure 5b the methyl proton signal for the label complex **13-^{13}C** is observed as a doublet of triplets because of the coupling with the ^{13}C nucleus (d, J_{CH} = 136.2 Hz) as well as the coupling with two magnetically equivalent ^{31}P nucleus (t, J_{PH} = 4.5 Hz).

NMR spectral data taken for **14a** are essentially the same as those for **13**. The ^{31}P{^{1}H} NMR spectrum of **14a** displayed two singlets at δ −3.9 and −4.8 due to the PPh_2 moieties. A triplet (δ 0.72, J_{P-H} = 4.8 Hz) assignable to the methyl group directly bound to the iridium center was observed in its ^{1}H NMR spectrum. We observed a broad resonance due to methyl groups of XylNC ligands at 35 °C, but lowering the temperature to −3 °C separated it into four singlets at δ 1.17, 1.33, 2.34, and 2.79 with the same intensity.

To our surprise, dichloromethane reacts with **5a**. Upon dissolving the Ir(I) complex **5a** in dichloromethane, $[Mo_2Ir_2(CH_2Cl)(Cl)(^t$BuNC$)_4$(pyphos$)_4](Cl)_2$ (**15**) was obtained in 72% yield (eq 7). The ^{31}P{^{1}H} NMR spectrum of **15** showed a pair of resonances at δ 2.0 and −2.3, in the same manner as **13**, and the ^{1}H NMR spectrum of **15** displayed a signal at

(36) Sanderson, R. T. *J. Am. Chem. Soc.* **1983**, *105*, 2259.
(37) Fedurco, M.; Sartoretti, C. J.; Augustynski, J. *J. Phys. Chem. B* **2001**, *105*, 2003.

Scheme 2

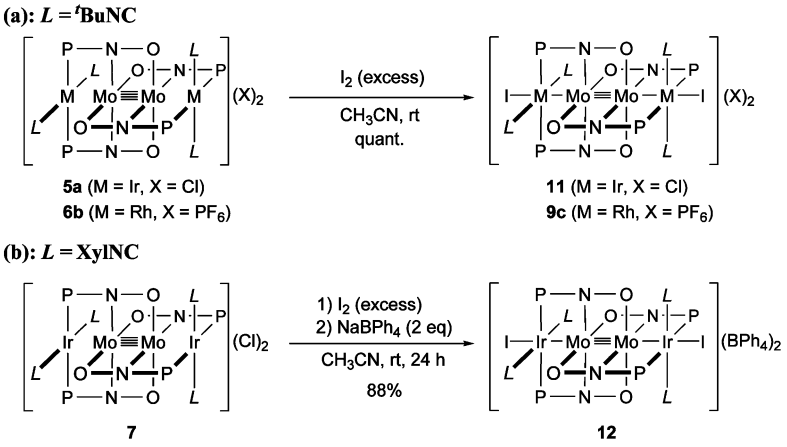

δ 3.94 attributable to the chloromethyl group coordinated to the one iridium center.

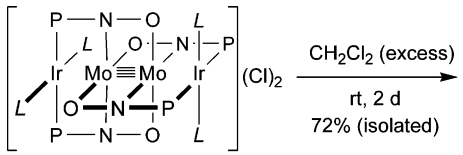

5a (*L* = ^{t}BuNC)

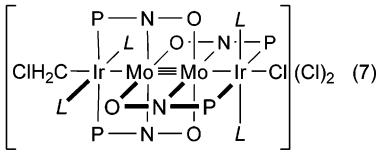

15

The molecular structure of the 1,4-oxidative addition product, $[Mo_2Ir_2(CH_3)(I)(XylNC)_4(pyphos)_4](BPh_4)_2$ (**14b**), which was obtained by treating **14a** with $NaBPh_4$, was determined by the X-ray diffraction study. However, as summarized in Table 4, the resulting crystal was found to be a mixed crystal consisting of two different cations, $[Mo_2Ir_2(CH_3)(I)(XylNC)_4(pyphos)_4]^{2+}$ involved in **14b** and $[Mo_2Ir_2(I)_2(XylNC)_4(pyphos)_4]^{2+}$ involved in **12**. X-ray diffraction analysis of this crystal revealed that the mixing ratio between the cationic parts of **14b** and **12**, that is the occupancy ratio between C79 and I6, was refined to 78:22. This ratio was further confirmed by combustion analysis. It is assumed that a part of the methyl iodide complex **14b** dissolved in dichloromethane gradually gave the diiodo species during recrystallization, resulting in cocrystallization with **12**. Figure 6 shows the ORTEP drawing of $[Mo_2Ir_2(CH_3)(I)(XylNC)_4(pyphos)_4]^{2+}$, and selected bond lengths and angles are listed in Table 4.

The linear Ir−Mo−Mo−Ir tetrametal framework is also retained completely. The methyl group (occupancy of 0.78) is located at one of the axial positions of the tetrametal skeleton with a bond distance of Ir2−C79 (2.090(12) Å), although I6 (occupancy of 0.22) is bound to Ir2 with a bond distance of 2.815(3) Å. The other iridium atom (Ir1) is ligated by an iodide atom (I5) with a full occupation factor with a bond distance of 2.8216(7) Å, almost the same as that of Ir2−I6. The distance of Mo1−Mo2 (2.1203(7) Å) is the same as that of the diiode complex **12** as well as the dichloro complex **10**. Both iridium metals adopt octahedral geometries, and the bond distances of Ir1−Mo1 (2.7805(6) Å) and Ir2−Mo2 (2.7466(6) Å) are comparable to those of **12**.

This X-ray analysis (the resulting crystal was found to be mixed with 22% of **12**) revealed that the electron-donating methyl ligand likely affects the length of the Ir(II)−Mo(II)−Mo(II)−Ir(II) core. The sum (7.584 Å) of bond distances of the two Ir−Mo bonds and the Mo−Mo bond in **12**, in which both axially extending coordination sites of the Ir(II) metals are occupied by iodine atoms, is equal to that in the dichloride complex **8** (7.588 Å); however, the corresponding value of 7.647 Å observed for the methyl iodide complex **14b** is significantly longer than that of **10** and **12**, most probably due to the trans influence of the methyl group.

Kinetic Study for the 1,4-Oxidative Addition of MeI toward the Linear Tetranuclear Ir(I)$_2$Mo(II)$_2$ Complex 5a. To elucidate the unique reaction mechanism of the selective 1,4-oxidative addition, kinetic analysis of the reaction of **5a** and CH_3I was performed. When several runs were performed under *not* pseudo-first-order conditions ($\alpha = [CH_3I]_0/[\mathbf{5a}]_0 < 10$), the absorbance−time curves were fitted to second-order equations (eqs 8 and 9), strongly suggesting that the 1,4-oxidative addition toward **5a** was first order in both **5a** and $[CH_3I]$.

$$-\mathrm{d}[\mathbf{5a}]/\mathrm{d}t = k[\mathbf{5a}][CH_3I] = k[\mathbf{5a}]\{(\alpha - 1)[\mathbf{5a}]_0 + [\mathbf{5a}]\} \quad (8)$$

$$[\mathbf{5a}]/\{[\mathbf{5a}] + (\alpha - 1)[\mathbf{5a}]_0\} = \exp\{-k(\alpha - 1)[\mathbf{5a}]_0 t\} \quad (9)$$

Kinetic analysis of the conversion of **5a** to **13** at different temperatures in acetonitrile under the pseudo-first-order condition using UV−vis spectrometry gave activation parameter values of 30(3) kJ mol^{-1} and −156(7) J K^{-1} mol^{-1} for $\Delta H^{\ddagger}$ and $\Delta S^{\ddagger}$, respectively (Figure 7 and Table 5). The highly negative value of the activation entropy was previously observed for the C−X bond activation as an indication of the highly ordered S_N2-type process.[38]

(38) Chock, P. B.; Halpern, J. *J. Am. Chem. Soc.* **1966**, *88*, 3511.

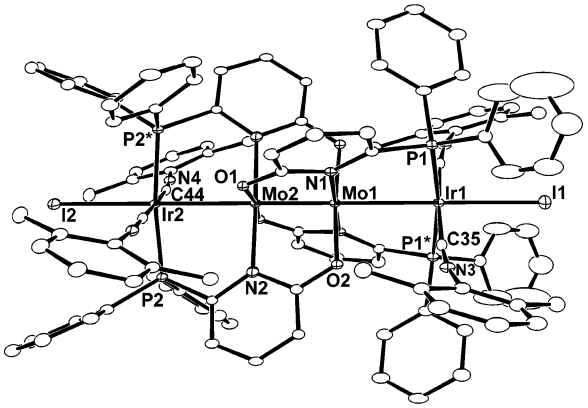

Figure 4. Molecular structure of **12** with thermal ellipsoids at the 30% probability level. H atoms, counteranions, and solvents are omitted for clarity.

Table 4. Selected Bond Lengths [Å] and Angles [deg] for **12** and **14b**[a]

	12	**14b**[a]
Mo1−Mo2	2.1249(9)	2.1203(7)
Mo1−Ir1	2.7427(8)	2.7805(6)
Mo2−Ir2	2.7161(8)	2.7466(6)
Ir1−I5		2.8216(7)
Ir2−C79		2.090(12)
Ir2−I6		2.815(3)
Ir1−I1	2.7760(8)	
Ir2−I2	2.7671(7)	
Ir1−P1	2.3476(15)	2.3418(12)
Ir2−P2	2.3403(14)	2.3365(12)
Ir1−C35	1.988(6)	1.961(5)
Ir2−C44	1.962(6)	1.959(5)
Mo1−O2	2.071(4)	2.083(3)
Mo1−N1	2.174(5)	2.186(4)
Mo2−O1	2.054(4)	2.065(3)
Mo2−N2	2.176(5)	2.181(4)
Mo2−Mo1−Ir1	180.0	180.0
Mo1−Mo2−Ir2	180.0	180.0
Mo1−Ir1−I1	180.0	180.0
Mo2−Ir2−C79	180.0	180.0
C35−Ir1−P1	86.41(17)	86.71(14)
C35−Ir1−P1*	93.82(17)	93.45(14)
C44−Ir2−P2	94.93(16)	94.95(14)
C44−Ir2−P2*	85.12(16)	85.11(14)
I5−Ir1−C35		89.09(13)
I5−Ir1−P1		94.83(3)
C79−Ir2−C44		89.47(13)
C79−Ir2−P2		93.66(3)
I1−Ir1−C35	88.32(16)	
I1−Ir1−P1	93.91(4)	
I2−Ir2−C44	89.64(15)	
I2−Ir2−P2	93.30(4)	
Mo1−Ir1−P1	86.09(4)	85.17(3)
Mo1−Ir1−C35	91.68(16)	90.91(13)
Mo2−Ir2−P2	86.70(4)	86.34(3)
Mo2−Ir2−C44	90.36(15)	90.53(13)

[a] C79:I6 = 0.78:0.22. Symmetry transformations used to generate equivalent atoms (*): $-x, -y, -z$.

The addition effect of TEMPO (2,2,6,6-tetramethylpiperidinooxyl radical) as a radical trap on the 1,4-oxidative addition was investigated to further examine the reaction mechanism. First, the control experiment of the reaction of **5a** in the presence of an excess amount (200 equiv) of TEMPO in acetonitrile at 30 °C generated unidentifiable products with λ_{max} value of 458 nm, and the pseudo-first-order disappearance rate constant of **5a** (k_{TEMPO}) was determined to be 1.17×10^{-4} s^{-1}. When the reaction of **5a** with CH_3I was performed at the same temperature in the presence of TEMPO (**5a**:CH_3I:TEMPO = 1:100:200) the disappearance rate constant of **5a** (k'_{obs}) was 8.74×10^{-4} s^{-1} (Table 5), almost equal to the sum of k_{obs} and k_{TEMPO} within experimental error, suggesting that a radical mechanism could be ruled out.

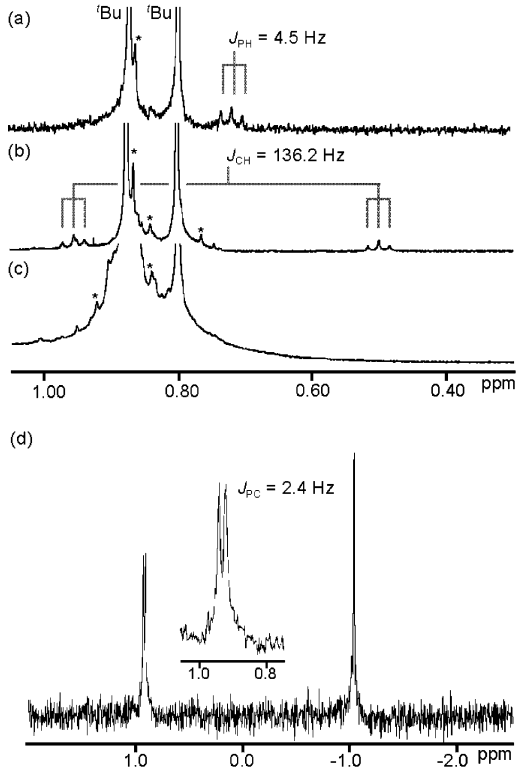

Figure 5. ^{1}H NMR spectra for (a) **13**, (b) **13**-^{13}***C***, and (c) **13**-d_3 showing the ^{t}BuNC and methyl ligand regions (300 MHz, CD_3CN, 35 °C). Asterisked signals represent unidentified impurities. (d) ^{31}P{^{1}H} NMR spectrum for **13**-^{13}***C*** (121 MHz, CD_3CN, 35 °C). The inset shows an enlargement to clarify the doublet signal centered at δ 0.9.

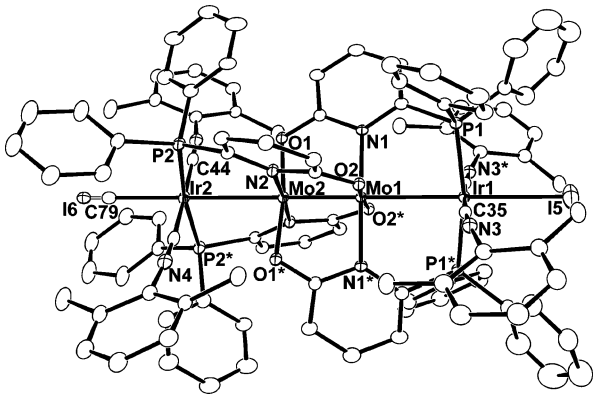

Figure 6. Molecular structures of $[Mo_2Ir_2(CH_3)(I)(XylNC)_4(pyphos)_4]^{2+}$ found in the crystal structure of the mixed crystal with thermal ellipsoids at the 30% probability level. H atoms, counteranions, and solvents are omitted for clarity. C79:I6 = 78:22

Discussion

Metal−Metal Bond Formation Mediated by Oxidation Reaction of M(I)$_2$Mo(II)$_2$ Tetranuclear Systems (M = Ir and Rh). The dimolybdenum quadruple-bonded complex **1** is a unique and versatile precursor for constructing heterometallic tetranuclear arrays because two pairs of trans-

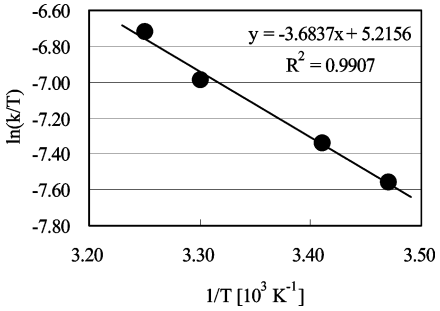

Figure 7. Eyring plot of 1,4-oxidative addition of CH_3I to **5a**.

arranged PPh_2 groups located at both axial sites of the Mo_2 core act as binding ligands for late transition-metal fragments. In this study we examined the introduction of M(I) (M = Ir and Rh) fragments into the $Mo_2(pyphos)_4$ system, and predictably, the geometries around each group 9 metal with chloro and carbonyl ligands in complexes **2** and **3** as well as their isocyanide derivatives **5**−**8** were square planar with planes perpendicular to the Mo−Mo vector (Figure 3a). As confirmed in the X-ray diffraction studies for **2**, **3, 5b**, and **6c** (Figures 1 and 2), the Mo−Mo bond distance in these $Mo(II)_2M(I)_2$ tetranuclear complexes is almost the same as that in **1**. The contribution of the direct σ-bonding interaction between the two M(I) atoms and the Mo_2 cores in these tetranuclear complexes is neglected. The same situation was observed in the M′(II)···Mo(II)−Mo(II)···M′(II) tetrametal arrays (M′ = Pt and Pd) (Scheme 3b)[18a] in which the square-planar geometry of the M′ metals is also perpendicular to the Mo_2 quadruple bond.

Chemical oxidation of two M(I) atoms to M(II) atoms was expected to be the key step for formation of the two M−Mo bonds, which induced the transformation of the geometry around the group 9 metals from square planar to octahedral (Scheme 3a). Oro et al., for example, reported that oxidation of rhodium atoms in several dinuclear M(I) complexes leads to formation of M(II)−M(II) single bonds,[19a] while partial reduction affords an infinite one-dimensional Rh chain molecule.[14] We succeed in oxidation of the isocyanide complexes **5**−**8** to give the corresponding M(II)−Mo(II)−Mo(II)−M(II) complexes **9**−**12** (Schemes 1 and 2, and eq 5), although the M(I) chloro carbonyl complexes **2** and **3** are oxidatively decomposed due to the prompt release of CO following treatment with oxidants such as $[Cp_2Fe][PF_6]$ and I_2. The X-ray diffraction studies for **9a**, **10**, and **12** clearly demonstrated formation of the Mo−M bond based on the short distances, which are suitable to forming a σ-bonding interaction. In this oxidation reaction the Mo−Mo bond order is formally changed from four to three with concomitant formation of two M−Mo bonds; however, we observe almost no variation in the Mo−Mo bond distance as well as the ν_{Mo-Mo} stretching,[39] while it should be expected (Table 6). The lack of variation is probably due to four quadruply bridging pyphos ligands, which bridge between the two molybdenum centers too tightly to give a flexible response to the change in the oxidation state or the metal−metal interaction at the terminal sites.

In order to achieve formation of the terminal M−Mo bonds, each terminal metal ion is required to have either d^7 or d^9 configuration with odd numbered electrons. In such cases, the terminal metal ions are allowed to have either octahedral or square-planar geometry in which one of the coordination sites is occupied by a molybdenum atom. Previously, we reported the syntheses of linear heterometallic clusters containing group 10 metals, and the key step of formation of $M'(I)_2Mo(II)_2$ metal arrays (M′ = Pd and Pt) such as $Mo_2Pd_2X_2(Pyphos)_4$ and $Mo_2Pt_2X_2(Pyphos)_4$ is reduction of two M′(II) metals of the corresponding precursors. The orientation of the two coordination planes of M′ atoms is dynamically transformed from perpendicular to coplanar to the Mo−Mo line, as schematically shown in Scheme 3b.[18a] In contrast, the metal−metal bonds of group 9 metal complexes are formed in a different manner: oxidation of M(I) metals led to formation of tetrametal arrays as a consequence of the change of the square-planar geometry of M(I) to the octahedral geometry of M(II).

1,4-Oxidative Addition of Alkyl Halides. Alkyl halides are commonly used for formation of carbon−metal σ-bonds via oxidative addition of the C−X bond toward low-valent transition-metal complexes,[40] and this oxidative addition is regarded as a key step for some catalytic processes.[41,42] This led us to investigate the oxidative addition of alkyl halides toward the tetrametal Ir(I)···Mo(II)−Mo(II)···Ir(I) complex **5a** as an alternative approach for constructing Mo−Ir bonds.

Treatment of CH_3I with the Ir(I) complex **5a** yields such an Ir(II)−Mo(II)-bonded tetrametal skeleton, which is the same as that obtained by chemical oxidation using $[FeCp_2]^+$ or I_2, but the terminal ligands are different. In the reaction the $Ir(I)_2Mo(II)_2$ core is formally oxidized by methyl iodide to give the $Ir(II)_2Mo(II)_2$ core with concomitant ligation of a methyl and an iodide ligand at the terminal sites of the tetranuclear framework. During the reaction no intermediates were detected with the corresponding homo-substituted diiodo and dimethyl products as evidenced from the spectral observation, thereby excluding the radical mechanism. Consequently, this unique and selective reaction of oxidants in the linear tetrametal clusters is the first example of a "1,4-oxidative addition" in which all four metals were bound linearly after formation of two Ir−Mo bonds and the bond order of the Mo_2 core is decreased.

(39) (a) Clark, R. J. H.; Franks, M. L. *J. Am. Chem. Soc.* **1975**, *97*, 2691. (b) Manning, M. C.; Holland, G. F.; Ellis, D. E.; Trogler, W. C. *J. Phys. Chem.* **1983**, *87*, 3083.

(40) (a) Milstein, D. *Acc. Chem. Res.* **1988**, *21*, 428. (b) Stille, J. K.; Lau, K. S. Y. *Acc. Chem. Res.* **1977**, *10*, 434. (c) Collman, J. P.; Hegedus, L. S.; Norton, J. R.; Finke, R. G. *Principles and Applications of Organotransition Metal Chemistry*; University Science Books: Mill Valley, CA, 1987; Vol. 2.

(41) (a) Forster, D. *Adv. Organomet. Chem.* **1979**, *17*, 255. (b) Forster, D.; Singleton, T. C. *J. Mol. Catal.* **1982**, *17*, 299. (c) Ellis, P. R.; Pearson, J. M.; Haynes, A.; Adams, H.; Bailey, N.; Maitlis, P. M. *Organometallics* **1994**, *13*, 3215.

(42) (a) Dickson, R. S. *Homogeneous Catalysis with compounds of Rhodium and Iridium*; D. Reidel: Dordrecht, The Netherlands, 1985. (b) Parshall, G. W.; Ittel, S. D. *Homogeneous Catalysis*, 2nd ed.; Wiley-Interscience: New York, 1992. (c) Cornils, B.; Herrmann, W. A. *Applied Homogeneous Catalysis with Organometallic Compounds (A Comprehensive Handbook in Two Volumes*); VCH: Weinheim, Germany, 1996.

Table 5. Kinetic Parameters for Reactions of **5a** with Substrate[a]

substrate (equiv)	k_{obs}/[s^{-1}][b]	$\Delta H^{\ddagger}$/[kJ mol^{-1}]	$\Delta S^{\ddagger}$/[J K^{-1} mol^{-1}]
CH_3I (100)	7.48×10^{-4} [c]	30(3)	−156(7)
TEMPO (200)	1.17×10^{-4} (k_{TEMPO})[d]		
CH_3I (100) + TEMPO (200)	8.74×10^{-4} (k'_{obs})[d]		

[a] In CH_3CN. [b] At 30 °C. [c] Average value of 5 runs. [d] Average value of 3 runs.

Scheme 3

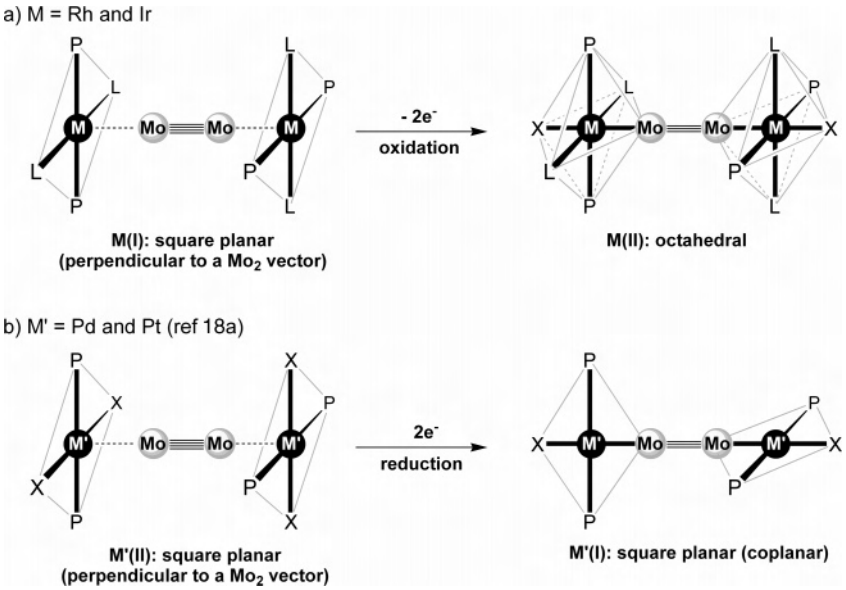

Table 6. Selected Resonance Raman Frequencies [cm^{-1}]

	ν_{MoMo}	d_{MoMo}/Å
1	394	2.098(2)
2	398	2.1115(9)
3	397	2.1087(7)
5a	396	
5b	392	2.1128(2)
6a	398	
6b	398	
6c	398	2.1054(6)
7	*a*	
8	391	
9a	388	2.1239(10)
9b	389	
9c	387	
10	388	2.1283(14)
11	387	
12	386	2.1249(9)
13	386	
14a	386	
14b	390	2.1203(7)
15	389	

[a] Complex **7** was decomposed during the measurement to change the color from blue-purple to red.

Furthermore, selective 1,4-oxidative addition of CH_2Cl_2 to **5a**, which results in formation of **15**, is surprising because activation of dichloromethane by mononuclear and dinuclear Ir(I) complexes, as far as we know, is rare.[43] It is noteworthy that the $Rh(I)_2Mo(II)_2$ analogue **6** can no longer react with alkyl halides, probably due to the difference in the nucleophilicity between iridium and rhodium.

Plausible Reaction Mechanism for 1,4-Oxidative Addition. Oxidative addition of oxidizing reagents to a d^8 square-planar late transition-metal center has been extensively studied for several decades.[40c,44−46] Three potential mechanisms for rationalizing the 1,4-oxidative addition of methyl iodide to **5a** are schematically shown in Scheme 4, where only the skeleton of the dicationic Ir_2Mo_2 unit is drawn and the ligands and anions are omitted for clarity. Path A involves η^1-coordination of methyl iodide to the one Ir(I) center followed by nucleophilic attack of the metal center by heterolytic cleavage of the C−I bond. Concurrently, the other Ir(II) center is attacked by an outer-sphere chloride anion, and soon after the chloride anion is replaced by an iodide anion. In common mononuclear d^8 square-planar complexes it is generally accepted that C−X and X−X bonds (X = halogen) are activated in an S_N2-like process, giving the trans-oxidative addition product.[47−50]

(43) (a) Tejel, C.; Ciriano, M. A.; Jiménez, S.; Oro, L. A.; Graiff, C.; Tiripicchio, A. *Organometallics* **2005**, *24*, 1105. (b) Marder, T. B.; Fultz, W. C.; Calabrese, J. C.; Harlow, R. L.; Milstein, D. *J. Chem. Soc., Chem. Commun.* **1987**, 1543.

(44) (a) Atwood, J. D. *Inorganic and Organometallic Reaction Mechanisms*, 2nd ed.; VCH Publishers: New York, 1997. (b) Atwood, J. D. *Inorganic and Organometallic Reaction Mechanisms*; Brooks/Cole: Monterey, CA, 1985.

(45) Rendina, L. M.; Puddephatt, R. J. *Chem. Rev.* **1997**, *97*, 1735−1754.

(46) Maitlis, P. M.; Haynes, A.; Sunley, G. J.; Howard, M. J. *J. Chem. Soc., Dalton Trans.* **1996**, 2187−2196.

(47) (a) van Koten, G. *Pure Appl. Chem.* **1990**, *62*, 1155. (b) van Beek, J. A. M.; van Koten, G.; Dekker, G. P. C. M.; Wissing, E.; Zoutberg, M. C.; Stam, C. H. *J. Organomet. Chem.* **1990**, *394*, 659.

(48) (a) Puddephatt, R. J. *Angew. Chem., Int. Ed.* **2002**, *41*, 261. (b) Aye, K.-T.; Canty, A. J.; Crespo, M.; Puddephatt, R. J.; Scott, J. D.; Watson, A. A. *Organometallics* **1989**, *8*, 1518.

(49) (a) Hughes, R. P.; Meyer, M. A.; Tawa, M. D.; Ward, A. J.; Williamson, A.; Rheingold, A. L.; Zakharov, L. N. *Inorg. Chem.* **2004**, *43*, 747. (b) Hughes, R. P.; Sweetser, J. T.; Tawa, M. D.; Williamson, A.; Incarvito, C. D.; Rhatigan, B.; Rheingold, A. L.; Rossi, G. *Organometallics* **2001**, *20*, 3800. (c) Hughes, R. P.; Ward, A. J.; Rheingold, A. L.; Zakharov, L. N. *Can. J. Chem.* **2003**, *81*, 1270.

Scheme 4

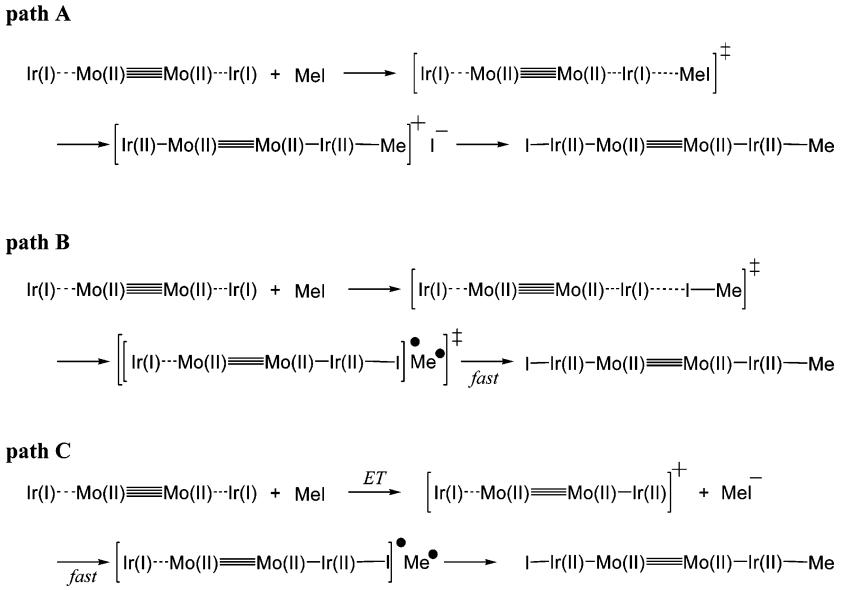

Path B, the so-called inner-sphere electron-transfer mechanism, involves one-electron oxidation of the iridium center by CH_3I, resulting in homolytic cleavage of the C−I bond. The next step is that the produced radical pair rapidly recombines to give the 1,4-oxidative addition product **13** before either species can escape from the cage. The rate of this type of reaction would be responsive to the C−X bond dissociation energy of the halocarbon, steric effects of the alkyl moiety, and halogen atom.[51]

Path C is an outer-sphere electron-transfer mechanism[52] involving one-electron transfer from **5a** to CH_3I at the initial stage to generate a CH_3I^- species, which undergoes fast dissociation to form a halide anion and a methyl radical.[53] The halide anion is trapped by one iridium center of the tetrametal species, and the methyl radical is caught by the other iridium center. It is reasonably assumed that oxidation of **5a** with 2 equiv of ferrocenium cation proceed via this electron-transfer mechanism. Turro et al. revealed that photoinduced one-electron reduction of alkyl halides by dirhodium tetraformamidinate complexes $Rh_2(L)_4$ (L = R-form, where R = *p*-CF_3, *p*-Cl, *p*-OCH_3, and *m*-OCH_3; form = *N*,*N*′-diphenylformamidinate) proceed via the outer-sphere mechanism, forming the corresponding halide complexes, $Rh_2^{5+}(L)_4-X$.[54]

Our electrochemical and kinetic measurements ruled out paths C and B for 1,4-oxidative addition of CH_3I to the Ir(I)···Mo(II)−Mo(II)···Ir(I) complexes because (1) path C is inconsistent with the redox potential values of CH_3I ($E_p^{0/-1}$ = ca. −2.7 V)[37] and **5a** ($E_{1/2}^{Ir(I)Ir(I)/Ir(II)Ir(II)}$ = ca. −0.97 V), which makes it more difficult for the electron transfer to occur between them, and (2) addition of TEMPO as a radical scavenger into the 1,4-oxidative addition reaction system did not affect the rate of the reaction, strongly indicating that this reaction is less likely to contain radical intermediates. Therefore, paths B and C were omitted.

Not only the negative activation entropy of −156(7) J K^{-1} mol^{-1} but also the observance of a second-order rate law in both concentrations of **5a** and CH_3I provide further evidence for an S_N2 mechanism (path A) for the 1,4-oxidative addition of CH_3I. In addition, the activation parameters of the reaction [$\Delta H^{\ddagger}$ = 30(3) kJ mol^{-1}, $\Delta S^{\ddagger}$ = −156(7) J K^{-1} mol^{-1}] are comparable to those observed for reactions between mononuclear group 9 complexes $[M(CO)_2I_2](AsPh_4)$ and CH_3I [M = Rh, $\Delta H^{\ddagger}$ = 50(1) kJ mol^{-1} and $\Delta S^{\ddagger}$ = −165(4) J K^{-1} mol^{-1}; M = Ir, $\Delta H^{\ddagger}$ = 54(1) kJ mol^{-1} and $\Delta S^{\ddagger}$ = −113(4) J K^{-1} mol^{-1}], which were reported to involve the S_N2 mechanism.[55]

A plausible reaction mechanism for 1,4-oxidative addition of methyl iodide to **5a** is thus concluded to be the S_N2 mechanism (path A), and more details are shown in Scheme 5. Formation of the η^1-methyl iodide adduct at the one axial Ir(I) center might occur in the S_N2-type mechanism. The concerted Ir(II)−Mo(II) bond formations, including cleavage of the C−I bond at the one iridium center and, at the same time, bond formation between the other iridium and the chloride anion, which was out of the coordination sphere, provided the intermediate complex where one of the axial positions was occupied by the methyl group and the other by the chlorine atom. The coordinated chlorine atom was successively and smoothly exchanged with iodide, resulting in formation of the selective 1,4-oxidative addition product **13**. The reactions of Ir(I)···Mo(II)−Mo(II)···Ir(I)

(50) Ruiz, J.; Lopez, J. F. J.; Rodriguez, V.; Perez, J.; de Arellano, M. C. R.; Lopez, G. *J. Chem. Soc., Dalton Trans.* **2001**, 2683−2689.
(51) (a) Halpern, J.; Maher, J. P. *J. Am. Chem. Soc.* **1964**, *86*, 2311. (b) Halpern, J.; Maher, J. P. *J. Am. Chem. Soc.* **1965**, *87*, 5361. (c) Chock, P. B.; Halpern, J. *J. Am. Chem. Soc.* **1969**, *91*, 582.
(52) Marzilli, L. G.; Marzilli, P. A.; Halpern, J. *J. Am. Chem. Soc.* **1970**, *92*, 5752.
(53) (a) Andrieux, C. P.; Merz, A.; Savéant, J. M. *J. Am. Chem. Soc.* **1985**, *107*, 6097. (b) Andrieux, C. P.; Gallardo, I.; Savéant, J. M.; Su, K. B. *J. Am. Chem. Soc.* **1986**, *108*, 638.
(54) Lutterman, D. A.; Degtyareva, N. N.; Johnston, D. H.; Gallucci, J. C.; Eglin, J. L.; Turro, C. *Inorg. Chem.* **2005**, *44*, 5388.
(55) Ellis, P. R.; Pearson, J. M.; Haynes, A.; Adams, H.; Bailey, N. A.; Maitlis, P. M. *Organometallics* **1994**, *13*, 3215−3226.

Scheme 5

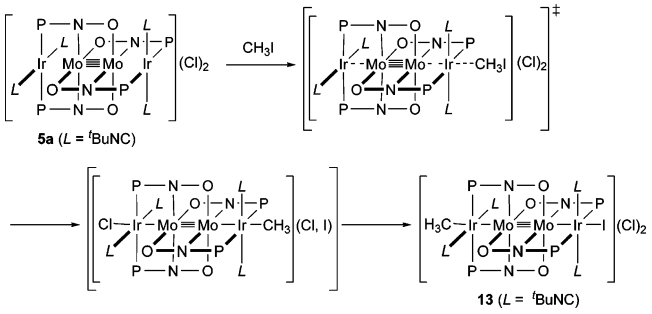

arrays with dichloromethane are also assumed to proceed via a similar S_N2 reaction pathway.

Reaction of **5a** with I_2 has two possible mechanisms, the S_N2 type or electron transfer, because the redox potential of I_2 is large enough to oxidize M(I) complexes. Reaction of **5a** with Br_2, which afforded an unidentified mixture, might be evidence for partial exclusion of the electron-transfer mechanism of the reactions of **5a** with X_2 because Br_2 is a stronger oxidizing agent than I_2 ($E^{0/-1}$ vs Fc/Fc^+: $Br_2 = 0.07$ V and $I_2 = -0.15$ V).[35] If reactions of **5a** with X_2 proceed via the electron-transfer pathway, treatment with Br_2 should smoothly afford the corresponding 1,4-oxidative addition product. Thus, the difference in reactivity between Br_2 and I_2 might arise from the bond dissociation energy (Br_2, 190.0 kJ mol^{-1}; I_2, 149.0 kJ mol^{-1})[56] rather than the oxidizing potential.

Conclusions

The quadruply bonded dimolybdenum complex $Mo_2(pyphos)_4$ (**1**) is a suitable precursor for constructing groups 6 and 9 heterometallic tetranuclear arrays because two pairs of trans-arranged PPh_2 groups located at both axial sites of the Mo_2 unit can act as a binding ligand for the d^8 group 9 metal, M(I), fragments. Oxidation of the introduced M(I) metals induces translation of the square-planar geometry of M(I) to the octahedral geometry of M(II) along with reduction in the bond order of the Mo_2 core to form the metal−metal-bonded tetrametal arrays. In addition to the chemical oxidation, the Ir(I) complex **5a** shows characteristic reactivity toward CH_3I and CH_2Cl_2, giving the corresponding 1,4-oxidative addition product $[Mo_2Ir_2(R)(X)(^tBuNC)_4(pyphos)_4](Cl)_2$ (**13**, R = CH_3, X = I; **15**, R = CH_2Cl, X = Cl) with the Ir(II)−Mo(II)−Mo(II)−Ir(II) skeleton. On the basis of the rate dependencies on the concentrations of both CH_3I and the Ir(I) complex **5a** and the observed activation parameters the mechanism for 1,4-oxidative addition reaction is the S_N2- type process observed for oxidative addition to mononuclear Ir(I) or Rh(I) complexes. Further studies will focus on the unique reactivity of the multinuclear complexes as promising candidates for constructing low-dimensional materials.

Acknowledgment. This work was supported in part by the Mitsubishi Science Foundation and JST, Japan Science and Technology Agency. A.S. thanks JSPS for supporting her postdoctoral fellowship (2006). We are grateful to Dr. T. Yamagata (Osaka University) for his contribution to the crystallographic analysis.

Supporting Information Available: Detailed experimental procedures and analytical and spectral data for complexes, kinetics, and crystallographic data (in CIF format) for **2**, **5b**, **10**, **12**, and **14b**. This material is available free of charge via the Internet at http://pubs.acs.org.

IC062474Q

(56) Huber, K. P.; Herzberg, G. *Molecular Spectra and Molecular Structure, IV. Constants of Diatomic Molecules*; Van Nostrand Reinhold: New York, 1979.